Vol. 396: 61–76, 2009
doi: 10.3354/meps08316

MARINE ECOLOGY PROGRESS SERIES
Mar Ecol Prog Ser

Published December 9

Dynamic 3-dimensional structure of thin zooplankton layers is impacted by foraging fish

Kelly J. Benoit-Bird*

College of Oceanic and Atmospheric Sciences (COAS), Oregon State University, 104 COAS Administration Bldg., Corvallis, Oregon 97331, USA

ABSTRACT: The potential attraction of fish to thin layers of zooplankton and the role of predation by fish in the formation and persistence of these layers were assessed using 3-dimensional sonar observations. Zooplankton were found in intense layers with vertical scales of 0.2 to 4.6 m with a mode of 2.2 m. These thin zooplankton layers had complex 3-dimensional structure with significant, though gradual, undulations in their depth, thickness, and intensity. Fish spent significantly more time within zooplankton layers than expected, modifying their usual surface-coupled behavior when layers were present. Sonar tracks of individual fish showed them diving down through a zooplankton layer before spiraling slowly upwards through the layer. The upward portion of this behavior was correlated with a dramatic decrease in the intensity of zooplankton scattering at the scale of 1 m^2, resulting in the appearance of holes in the layer. Continued observation of layers revealed that these holes slowly filled in with zooplankton an average of 4.3 min after the fish's departure. Survey results show that when more fish were observed, more holes were observed, and when larger fish were observed, larger holes were observed, so that a total of up to 5% of a layer's area could be comprised of holes. The thickness of layers was not affected by fish presence. Fish were attracted to zooplankton thin layers, showing that thin layers in natural systems can have significant ecological effects; however, despite fish-associated changes to the structure of layers, the layers were resilient over time to the apparent foraging fish.

KEY WORDS: Thin plankton layer · Fish · Foraging · Behavior · Multibeam echosounder

INTRODUCTION

The distribution of organisms in the ocean is highly heterogeneous, influencing both sampling and ecological structure. The complex spatial and temporal structures of predators and prey affect one another. Predators tend to congregate in areas of high prey density (Krebs 1978) while prey are trying to avoid or escape predators. Many animals, including marine mammals (Fiscus & Kajimura 1981, Fertl et al. 1997, Merrick et al. 1997, Barros & Wells 1998, Tamura et al. 1998, Benoit-Bird & Au 2003), water birds (Cairns 1987, Greene 1987, Burger et al. 1993, Burkett 1995, Ostrand et al. 1998, Cherel et al. 1999), and fishes (Roger 1994, Krause & Godin 1995, Buckel et al. 1999) feed specifically on schooling or aggregated aquatic prey. This phenomenon seems to be particularly widespread when the prey is pelagic. The density and distribution of an animal's food resource in its immediate surroundings determine the amount of food the animal can obtain in a brief period, affecting its growth and survival (Beyer 1995) as well as its behavior (Benoit-Bird & Au 2003).

A predator's survival is impacted over the long term by its prey, while, conversely, a prey organism's survival is immediately impacted by its predator. Predation risk can affect the foraging behavior of the prey species (Lima & Dill 1990) and can even induce physiological and morphological changes in prey (Brönmark & Miner 1992). Predators can affect prey density through direct predation as well as prey emigration, since prey select different habitats in response to pre-

*Email: kbenoit@coas.oregonstate.edu

dation risk (Kratz 1996), ultimately impacting community composition (Cooper et al. 1990). Prey in benthic systems have been found to aggregate into discrete patches as a mechanism to avoid predators (see, for example, Hildrew & Townsend 1982), changing not only the prey animals' density but also their distribution. While numerous studies in pelagic systems have investigated the effects of prey distribution on predator behavior, and studies in benthic habitats have revealed the significant impacts predators can have on prey distribution (see a review in Cooper et al. 1990), relatively few field studies outside the schooling fish literature have investigated the effects of predator behaviors on prey distribution in pelagic systems (Orr 1981, Axelsen et al. 2001, De Robertis et al. 2003, Benoit-Bird & Au 2009). These interactions can have effects on individual animals, their competitors and predators, as well as the measurements obtained of them and their environment.

Recent advances in measurement capabilities have led to the discovery of an extreme example of heterogeneity in the plankton; aggregations over continental shelves with vertical dimensions of tens of centimeters. These 'thin layers' can have a horizontal extent of several kilometers and may persist for days (Dekshenieks et al. 2001, Rines et al. 2002, McManus et al. 2003). Sharply distinct from the surrounding water column, these layers contain a density of phytoplankton and zooplankton significantly higher than at surrounding depths (Cowles 2003).

The ubiquity of thin layers of plankton in coastal ecosystems (Cheriton et al. 2007) hints at their ecological importance. However, field studies investigating the ecological consequences of thin plankton layers have been limited. It is likely that planktivores will be attracted to these narrow-depth regions of aggregated plankton, as hypothesized by Lasker (1975). Laboratory studies have shown that thin layers of zooplankton directly influence the vertical distribution of larval herring, suggesting an attraction of zooplanktivores to these areas of abundant resources despite their preference for other depths (Clay et al. 2004). Modeling results suggest that a predator's efficiency inside an even and continuous thin layer is decreased relative to foraging in a patchy thin layer, effectively decreasing the prey's risk (Leising 2001). Thus, it is possible for organisms to reduce their predation risk within thin layers by changing their horizontal aggregation, suggesting that predators can have a significant impact on the horizontal distribution of layers. Predation probably has significant impacts on the vertical distribution of thin layers as well. Donaghay & Osborn (1997) suggested that feeding on thin layers could be a significant source of prey mortality, leading to degradation of the layers. Alternatively, feeding on the layer from above or below may actually create sharp edges to the layer, aiding in its formation or maintenance (Donaghay & Osborn 1997). An understanding of predator presence and layer use is critical for understanding how thin layers are formed, maintained, and dissipated, and is an important step towards understanding the role of these features in coastal marine ecosystems. The goals of this work were to: (1) measure the scales of thin zooplankton layers in 3 dimensions; (2) determine the potential role of fish in determining these scales; and (3) assess the role of zooplankton layers as a potential resource for fish by measuring zooplankton and fish behavior in and around thin layers.

MATERIALS AND METHODS

Observations of zooplankton and fish were made using shipboard acoustics during both underway and stationary sampling. Previous studies have shown that acoustical approaches are quite useful in monitoring small-scale zooplankton features (Holliday et al. 1998, 2003, McManus et al. 2003, Cheriton et al. 2007). These acoustic data were supplemented by visual observations and vertical net tows. Data were collected in Monterey Bay, California, during 2 time periods in the summer of 2006. From 13 to 27 July 2006, sampling was conducted during daylight hours as part of the Layered Organization in the Coastal Ocean (LOCO) project in and around the experiment's mooring array that ran in a line from 36.9381° N, 121.9171° W to 36.9273° N, 121.9283° W. Frequent surveys covered a 5 km transect running approximately 1 km inshore of the shallowest mooring to 2 km offshore of the deepest. Stationary observations were made periodically, usually in the areas surrounding each of the experiment's 4 mooring sites. The selection of stationary sampling sites was based on the needs of other investigators using the vessel as well as data from optical and acoustical sensors. From 4 to 8 August 2006, nighttime sampling was conducted in the same general area, with underway sampling of a 3 km across isobath by 2 km along isobath box, along with 20 min stationary observations at each of the corners of the box on every pass. All underway surveying was conducted at a vessel speed of approximately 9 km h^{-1} (5 knots). During both studies, underway sampling with the multibeam echosounder provided 3-dimensional information on both thin zooplankton layers and fish that can be analyzed statistically. Stationary sampling from both studies allowed a 4-dimensional analysis of layers and fish through repeated sampling of approximately the same volume.

Direct sampling. During all daytime sampling, visual observations of fish near the surface and those in the

mouths of seabirds and sea lions were made at intervals of 5 min. The observations were made by an individual experienced with identifying the species found in Monterey Bay. Fishermen were also informally interviewed daily at the docks to determine the most abundant fish present in the bay throughout the study.

During daytime and nighttime sampling, vertically integrated plankton tows were conducted using a 0.75 m diameter 333 µm mesh equipped with a General Oceanics flowmeter. A total of 49 tows were conducted from 3 m above the bottom to the surface. Plankton samples were preserved in 5% buffered formalin in seawater and were later identified to genus, measured, and enumerated.

Acoustic sampling. The transducers of a 38 and 120 kHz split-beam echosounder (Simrad EK60s) were mounted 1 m beneath the surface on a rigid pole off the side of the RV 'Shana Rae'. The 38 kHz echosounder had a 12° beam and used a 256 µs pulse with an input power level of 800 W. The 120 kHz echosounder had a 7° beam and used a 64 µs pulse with an input power of 200 W. The goal of the combination of instruments was not to create 'combined frequency data' to facilitate species identification (Korneliussen et al. 2008) but rather to exploit the strengths of each instrument while providing the high vertical resolution necessary for addressing the scales of plankton thin layers. Both echosounders were calibrated in the field using an indirect procedure incorporating a 38.1 mm diameter tungsten carbide reference sphere as prescribed by Foote et al. (1987), using the same setup used for the study. For calibration, the reference sphere was held at varying distances from 3 to 22 m with nearly identical mean target strengths measured by both frequencies at all ranges with no systematic change in target strength as a function of depth. This suggests that non-linear effects are negligible in the setup used over the depth range where observations were made (Tichy et al. 2003).

The transmit and receive transducers of the 200 kHz multibeam echosounder (Simrad-Mesotech SM2000) were mounted to a small rotating motor controlled by a topside computer before being mounted next to the echosounder transducers. This allowed the multibeam echosounder to be rotated fore and aft during stationary sampling and to be pointed directly downward during underway sampling. During stationary observations, the motor rotated the multibeam echosounder transducers over a ±20° range from the vertical over a period of 15 s before reversing rotation. This permitted later reconstruction of the scattering field in 3 and even 4 dimensions despite the lack of vessel motion.

The multibeam echosounder had 120 $1.5° \times 20°$ beams that overlapped by 0.25° in the across-track direction, providing an angular coverage 120° with 1° resolution in this direction. Data were taken using the external imaging transducer of the sonar, thus forming a Mills Cross to provide the greatest spatial resolution. This gave a received beam width of 1.5° in the along-track direction. The system had a vertical resolution of 0.20 m. The multibeam echosounder used a 150 µs outgoing pulse transmitted at a rate of 5.6 s^{-1}, with an input power of 80 W. The multibeam echosounder system was calibrated in the Applied Physics Laboratory of the University of Washington's seawater calibration facility using tungsten carbide spheres with diameters of 20 and 38.1 mm following the protocols established by Foote et al. (2005). The system showed a nearly linear gain function, stable performance, and beam patterns consistent with those predicted by the system geometry.

A small, 0.05° accuracy tilt-and-roll sensor was mounted to the plate holding the echosounder transducers to provide data on vessel motion. These data and differential GPS data were digitized simultaneously with raw echo data from the split-beam and multibeam echosounders. Most sampling was conducted with sea states below Beaufort 2 (waves of less than 0.2 m, winds below 6 knots), often with completely glassy conditions, limiting undesirable vessel movement.

Echosounder data analysis. Scattering from the areas surrounding any probable schools of fish (e.g. discretely bounded, intense, relatively evenly scattering in 38 and 120 kHz, ovoid or otherwise non-layered aggregations) were excluded from further analysis because previous work showed schools were not associated with zooplankton layers (Benoit-Bird et al. 2009). Single targets in each echosounder frequency (i.e. large individual scatters at densities equal to or less than 1 per sampling volume) were extracted using SonarData's Echoview program using a target strength threshold of −70 dB. A pulse length determination level (the value in dB below peak value considered when determining the pulse length, or envelope, of a single-target detection) of 12 dB was used. Normalized pulse lengths (the measured pulse length divided by transmitted pulse length) were required to be between 0.8 and 2.0. The maximum beam compensation for correcting transducer directivity was set to 12 dB. To confirm all sources of scattering within the measured pulse length were from a single target, all samples within this pulse envelope must have had a standard deviation in angular position of less than 3° in both the along and athwart ship directions of the beam. Identified single targets were later analyzed independently.

For analysis of volume scattering data, the scattering from single targets must be removed. Single targets were masked in all frequencies, similar to the approach of Jurvelius et al. (2008). The scattering from single targets was basically replaced with no value, so that their

scattering did not affect volume scattering measurements, which must be calculated using averaging. The parameters used to detect single targets for analysis of fish characteristics were very conservative, possibly missing fish that should not be included in the volume scattering analysis. Two approaches were taken to address this. First, the single-target parameters were relaxed so that the normalized pulse lengths could be between 0.25 and 4.0. Targets identified with this expanded range that were greater than –70 dB were also masked to remove them from the volume scattering analysis; however, they were not included in the analysis of the characteristics of single targets. Second, the difference in scattering between 38 and 120 kHz of individual 1 m × 1 m cells was examined. Any values between 3 and –3 dB, consistent with scattering from fish, were excluded from volume scattering analysis. The number of these additional potential fish targets from both methods was less than 1% of all samples. An ANOVA on the rates of detection of these potential targets showed no significant effect of sampling date, depth, or layer presence ($p > 0.10$ for all comparisons). This suggested that their removal has a limited effect volume scattering analysis. After exclusion of these potential fish targets, the remaining volume scattering data were averaged over 5 contiguous echoes for comparison with the multibeam echosounder data.

Multibeam data analysis. Data from the multibeam echosounder were beamformed with Chebyshev-type amplitude weighting, and the amplitude and range of echoes in each beam were then extracted using a custom MATLAB program (The MathWorks). Single targets in the multibeam echosounder data were identified using a custom MATLAB program using the same criteria used for the split-beam echosounders. Scattering from single targets was then removed from the data for independent analysis. Similarly, the scattering from targets identified using the relaxed pulse length values were also excluded from the volume scattering analysis. The remaining volume scattering was averaged over 5 beams across-track and 5 echoes along-track with no vertical averaging and then thresholded at a value of –75 dB. This provided spatial resolution at a depth of 10 m, approximately the mode of detected layers, of about 1 m both across and along track during stationary sampling, and 1 m across and 2.5 m along track during underway sampling. This provided adequate averaging for volume scattering estimation while still providing a vertical resolution of 0.2 m. The range versus azimuth data from both single targets and mean volume scattering were transformed into a rectangular coordinate system, and the vessel motion was removed using both the GPS and tilt-and-roll data.

Single target analysis. Single targets with target strengths greater than –70 dB were consistent with scattering from individual small fish. The frequency differences in target strength of single targets identified within the beam of both the 38 and 120 kHz split-beam echosounders support this interpretation with relatively small frequency differences. The differences were much lower than expected from zooplankton echoes, which, over the range of frequencies used here, are more frequency-dependent than those from fish (Korneliussen & Ona 2002).

To calculate the depth distribution of individual fish, the number of single-target detections from underway surveys was corrected for search area differences as a function of depth (caused by the conical shape of the transducer's beam). This was done by dividing the number of animals located at a particular depth by the diameter of the beam at that depth. Diameter, not area, of the beam was used, because the second dimension of the beam is covered by the direction of the transect. Counts of individual fish in survey data were conducted only for the area within 5 m vertically of the peak of an identified thin layer. This was done in order to reduce the inclusion of fish associated with the surface and not the thin layer in this relatively shallow water column, resulting in an average volume of approximately 10000 m^3. These counts were then converted to density for comparison with thin layer characteristics by dividing by the total volume of water sampled within 5 m of a thin layer. The density of all single targets within the water column was similarly calculated when layers were detected and when they were not for comparison of fish vertical distributions.

Thin layer definition. Following the definition of Cheriton et al. (2007), thin layers were identified as features less than 5 m thick and at least 3× (4.75 dB) greater in intensity than the background volume scattering. The background was defined by calculating a vertical 5 m running median at each x,y position in the processed volume scattering data. Each layer's peak was defined as the depth of its most intense scattering value and its minimum and maximum depths as the points above and below this depth, respectively, where the scattering first fell below the running median value. The thickness of the layer was calculated as the range of values within half the peak intensity of the layer, sometimes called the full width half maximum (FWHM).

Layer gradients. To quantify thin layer gradients, the distance between the edge of the layer and its peak were divided by the change in the intensity of layer's acoustic scattering in linear units over that depth, resulting in a measure in m σ^{-1}. This value approaches 0 when a layer is extremely sharp, while a more gradual increase in scattering intensity results in a higher, positive number. An average gradient for the upper and lower edges was calculated for each 50 m along

track section of thin layers detected with the multibeam echosounder.

Relative surface area. To quantify the 3-dimensional structure of the top and bottom edges of identified thin scattering layers, a relative surface area calculation was made for data collected with the multibeam echosounder. At the average depth of identified thin layers, the multibeam echosounder's across-track field of view is approximately 50 m. To provide roughly equivalent analysis in the along-track direction, multibeam echosounder data from 50 m long sections of underway transect were analyzed. Because of differences in the along-track sampling area with depth, direct measures of surface area could not be made. Instead, the area of a linearly interpolated surface connecting all the minimum layer depths within each 50 m transect section were compared to the area of a flat, level sheet at the mean of the depth minima in the same area (Fig. 2C). This results in a value of 1 for a very smooth, level thin layer and positive values representing increased tilt and rippling of the layer. A similar calculation was conducted for the lower edge of each thin layer.

Diel/date patterns. Diel patterns could be important to the interpretation of results of this study. However, because of the sampling design, which was constrained by the needs of other investigators, daytime and nighttime sampling were conducting during different time intervals. This meant that time of day and date of sampling covaried, making it impossible to separate their effects. To assess if diel patterns may affect interpretation of the data, multivariate analyses of variance (MANOVAs) on the effect of date were carried out on the characteristics of layers and single targets. To reduce the chance of type 1 or false-positive error, the critical p value was raised to 0.10 from the customary 0.05.

RESULTS

Fish observations

Fish were frequently observed visually in the upper water column during daytime sampling. These observations of fish at the surface and those being foraged on by seabirds and sea lions indicated that the dominant fish species in Monterey Bay during 2006 were Pacific sardine *Sardinops sagax* and northern anchovy *Engraulis mordax*. Interviews with commercial purse seine fishermen in Monterey Bay confirmed that they were also catching primarily sardines and anchovies. Both observations and informal interviews suggested that Pacific sardines were numerically dominant over northern anchovy in Monterey Bay. This is supported by the commercial landings reported by the California Department of Fish and Game for the greater Monterey Bay area. These landings showed that, of pelagic fish landed during the study period, 64% were Pacific sardine, 33% were northern anchovy, and 3% were other small fish, primarily Pacific herring.

Zooplankton

In the 49 net tows conducted, zooplankton were dominated by copepods both numerically and by biomass. The most abundant genera of copepods were *Calanus* (mean body length = 1.35 mm ± 0.27, mean ± SD), *Ctenocalanus* (mean length = 0.88 mm ± 0.09 SD), and *Acartia* (mean length = 0.95 mm ± 0.07, mean ± SD). Together, these 3 groups made up more than 90% of the zooplankton both numerically and by biomass. Only copepods were numerically abundant enough to allow comparison of their mean density from net tows taken within areas with detected thin layers with those taken in areas without layers. An ANOVA for the effects of layer presence on copepod density in net tows showed a significant effect ($F = 37.86$; df = 1,47; $p < 0.001$). The samples collected from areas with thin zooplankton layers had a mean density of 71.4 copepods m^{-3}, about 68 copepods m^{-3} greater than the mean of 3.1 copepods m^{-3} in tows from areas without thin layers. If the background densities of copepods are equal in the presence and absence of layers, the average layer would have had to have a density of approximately 1000 copepods m^{-3} to account for the differences in copepod density observed in the net tows.

Underway sampling

During underway sampling, a total 394.6 km were surveyed, and 139.1 of these km had zooplankton thin layers. During the main LOCO experiment, when daytime sampling was conducted, layers were detected 16.1% of the time, with multiple layers occurring in the same location 1.8% of the time. During the nighttime sampling following the main experiment, layers were detected 50.2% of the time, with more than one layer occurring in the same location 23.9% of the time. The typical frequency response of these layers is apparent in an example layer shown in Fig. 1. Scattering of all identified layers was at least 13 dB less at 38 kHz than at 120 kHz, with differences between 20 and 30 dB observed in more than 80% of layers. While surveys showed that these layers were often extensive, covering kilometers continuously, layers varied greatly in their vertical structure and intensity. One example is

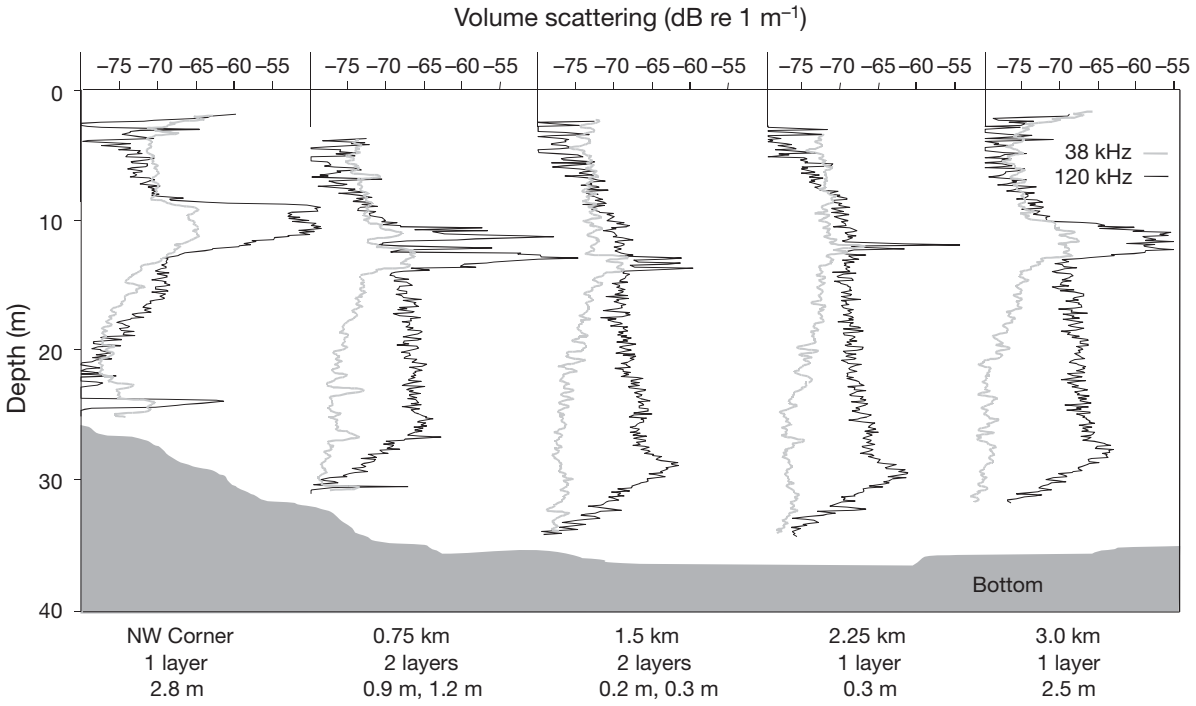

Fig. 1. Volume scattering strength at 38 kHz (gray lines) and 120 kHz (black lines) as a function of depth at 5 locations along a 3 km long transect running offshore. The number of thin scattering layers identified in the 120 kHz data is shown below each plot, along with the thickness of the layers in order from shallowest to deepest. Despite the fact that this feature was continuous along the entire transect, there is considerable variability in the profile of the layer along this distance. The scattering at 38 kHz often shows a local peak in scattering at the position of the layer identified in the 120 kHz data; however it is typically reduced by 15 to 30 dB relative to the scattering at 120 kHz, a change equal to a 30- to 1000-fold difference, as it is in the examples shown here

shown in Fig. 1. Note how this continuous feature splits into more than one layer and changes thickness over the 3 km transect. Even within a single echo return from the multibeam echosounder, there was considerable variation in layer depth and structure. The upper panel of Fig. 2 shows data from the multibeam echosounder averaged over 1 m along track and 5 pings. The lower panel shows the complexity of the same layer's shape over 8 m along the track of the vessel.

Single targets were detected quite often within the study area. The difference in target strength between targets detected at 38 kHz and those detected at 120 kHz from the split-beam echosounders was between 3 dB and −3 dB for all targets detected with a threshold of −70 dB, consistent with scattering from fish rather than zooplankton (Kang et al. 2002, Korneliussen & Ona 2003). In an effort to identify fish that may have been aggregated but should still be excluded from analysis of volume scattering in thin layers, 2 approaches were utilized. First, less stringent echo criteria were used for single target detection. This did not substantially increase the number of detected single targets. Second, the frequency response of each 1 m × 1 m cell in the split-beam echosounder data was examined, and those cells showing a frequency response similar to the response observed for single targets were excluded from volume scattering analysis. Combined, these 2 approaches identified potential fish missed by the initial single target analysis in less than 1% of cells within the data. Because of the small number of data points affected by these analyses and the lack of any effects of date, depth, or layer presence on their detection rate, their removal was not likely to bias the results.

The effects of sampling date were assessed on the observed characteristics of zooplankton thin layers using MANOVA (Table 1). Similarly, MANOVA was

Table 1. Multivariate analysis of variance (MANOVA) of the characteristics of thin zooplankton layers as a function of sampling date. Because of the sampling design, time of day and date cannot be separated, and thus a non-significant date effect can also be interpreted as a non-significant diel effect

Layer variable	df	Error df	*F*	p
Thickness	17	2781	0.563	>0.1
Depth	17	2781	0.988	>0.1
Surface area	17	2781	0.822	>0.1
Upper gradient	17	2781	0.775	>0.1
Lower gradient	17	2781	0.971	>0.1
Hole area/layer area	17	2781	0.475	>0.1
Layer mean intensity	17	2781	3.773	0.06

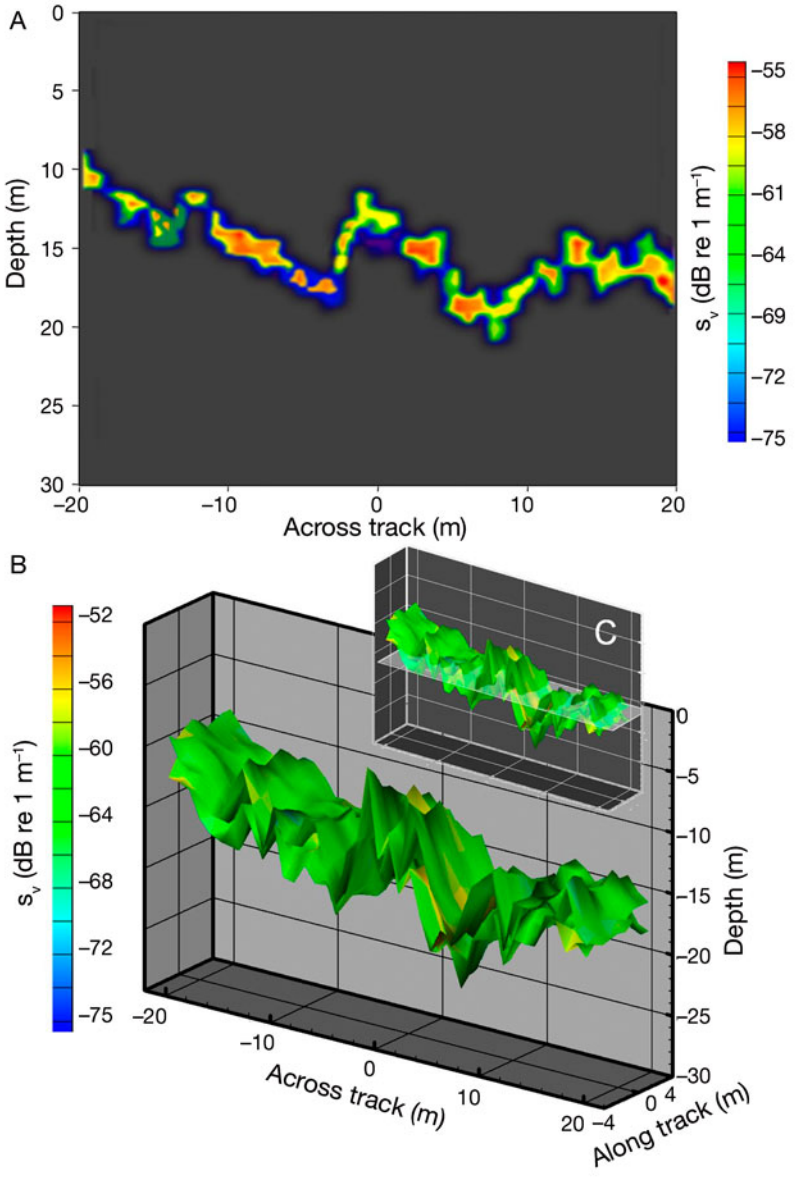

Fig. 2. (A) Volume scattering from the 200 kHz multibeam echosounder. Data are an average of 5 echoes covering approximately 1 m along the vessel's path and are averaged over 1 m bins across the vessel's path. (B) 3-dimensional rendering of the same data, along with 8 other similar volume scattering measurements made at 1 m increments along the track of the vessel's motion. (C) Conceptual drawing of how the relative surface area of a layer is calculated. It is an identical rendering of the data with a flat plane shown at the mean depth of the layer. The area of the top and bottom edges of the layer are divided by the area of the flat plane to determine the relative surface area

used to examine the effect of date on the characteristics of detected single targets, shown in Table 2. Because of constraints on the sampling design, sampling during the day was conducted only during the July sampling interval. Sampling at night was only conducted during the August sampling, making it impossible to separate the effects of diel patterns from those of date. However, there were no significant effects of date on any layer characteristic except layer intensity. There were also no observed effects of date on single-target characteristics, suggesting no diel effects on these features. MANOVAs pooling date into July and August only did not change the results (data not shown). As a result, all data from the 2 study periods were pooled for the remaining analyses.

Mean layer thickness was measured from the multibeam echosounder data in 50 m bins along survey transects. A histogram of layer thickness from underway sampling is shown in Fig. 3. It is important to note that there are very few layers thicker than 3.6 m, validating the use of 5 m as a cutoff for defining layers in this data set. The thinnest layers that could be measured were 0.2 m, the vertical resolution of the multibeam echosounder. Of the 2782 sections (50 m) of multibeam echosounder that contained zooplankton thin layers, 48% also contained single targets consistent with fish, while 52% did not. ANOVA showed that there was no significant effect ($F_{1,2781}$ = 1.351; p > 0.05) of single-target presence on layer thickness.

Fig. 4 shows a histogram of the depth of all acoustically identified zooplankton thin layers from the multibeam echosounder data (n = 2782). ANOVA showed no significant effect of single-target presence on layer depth ($F_{1,2781}$ = 0.448; p > 0.05). Fig. 4 also shows a histogram of the depth of single targets when layers were present (n = 1335) and the depth of single targets when no zooplankton layer was detected (n = 1855). A *t*-test revealed that there was a significant effect of layer presence on the depth of single targets (t = 3.814; df = 3188; p < 0.001).

Single targets from the multibeam echosounder were consistently found associated with the bottom edge of zooplankton thin layers, as shown in Fig. 5. Note that this figure only shows depths of individual fish that were within the 95% confidence interval around the mean depth relative to the layer's bottom edge for simplicity. It excludes targets that may have been swimming down to or coming up from the layer. Stationary observations indicated that swimming down to and up from the layer represents only a small fraction of an individual target's time (see data visualization movie in electronic supplement at www.int-res.com/articles/suppl/m396p061_app/). The focus of in-

Table 2. MANOVA of the characteristics of detected single targets as a function of sampling date. Because of the sampling design, time of day and date cannot be separated, and thus a non-significant date effect can also be interpreted as a non-significant diel effect

Single-target variable	df	Error df	*F*	p
Target strength	17	3188	0.123	>0.1
Depth	17	3188	0.599	>0.1
Numerical density	17	7891	0.959	>0.1

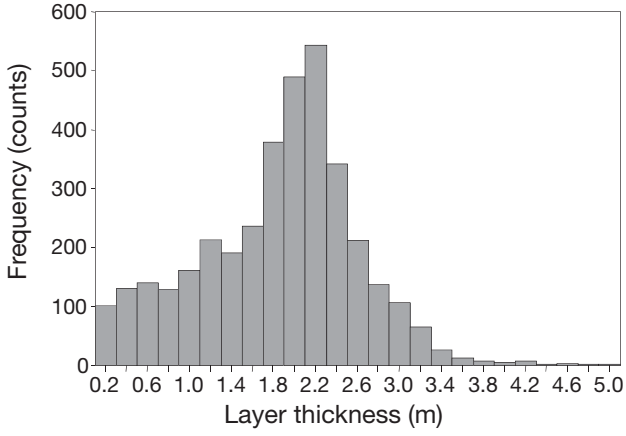

Fig. 3. Histogram of the thickness of all thin acoustic scattering layers identified during underway sampling. Thickness was measured as the vertical distance between the points about each layer's peak that were half of the peak volume scattering value. The thinnest layers that could be measured given the multibeam echosounder's vertical resolution were 0.2 m

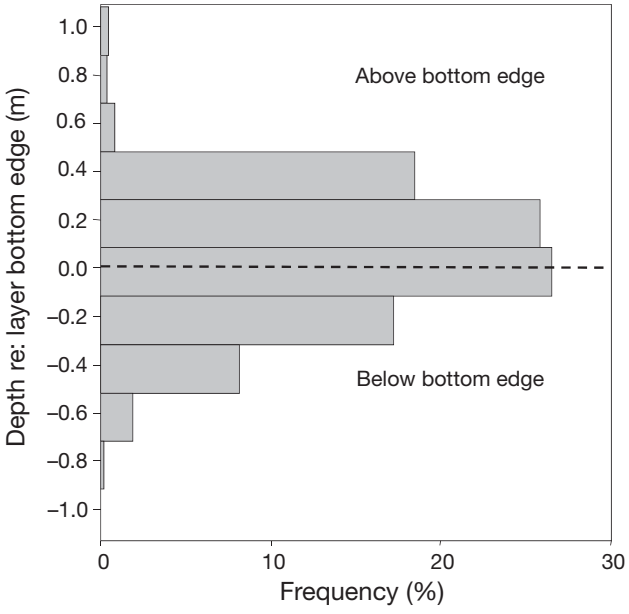

Fig. 5. Depth of individual targets detected with the multibeam echosounder within 5 m of the edge of a simultaneously identified thin layer during underway sampling. Depth is shown relative to the bottom edge of the layer defined as the point that the intensity below the layer's peak falls below the 5 m running median value. Depth of individual targets was corrected for beam effects by dividing the counts of single targets by the diameter of the beam at that depth. Only depths relative to the bottom edge that were within the 95% confidence interval about the mean are shown

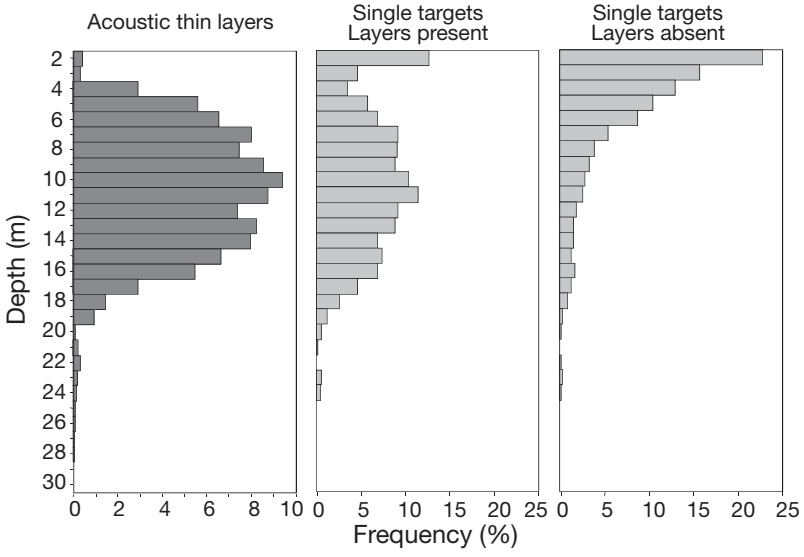

Fig. 4. Left: Histogram of the depth of all acoustically identified thin layers from underway sampling. Water depth ranged from approximately 20 to 30 m. Center and right: Histograms of the depth of single targets identified during underway sampling, showing single targets detected when thin layers were also detected (center panel) and single targets when no thin layers were identified (right panel). There was a significant effect of thin zooplankton layer presence on single-target depth

of individual targets on the layer's bottom edge appears to have a significant effect on layer characteristics. Fig. 6 shows relative surface area (an estimate of the 3-dimensionality of a thin layer's edges) as a function of the density of fish in the 5 m around the layer. The slope of the regression for the layer's top edge was not significantly different from 0 ($p > 0.05$), while there was a significant effect of fish density around the layer on the structure of the bottom edge of layers detected during underway sampling ($r^2 = 0.58$; $p < 0.01$). Similarly, as shown in Fig. 7, the gradient of the layer's top edge was not related to the density of fish in the 5 m surrounding the layer, as the slope of the regression was not significantly different than 0 ($p > 0.05$). The gradients of the layer's top edges were all quite small, representing a sharp transition between the layer and the background, regardless of the density of fish. This was not the case for the bottom edges of layers, which were much less distinct from the background when fish were pre-

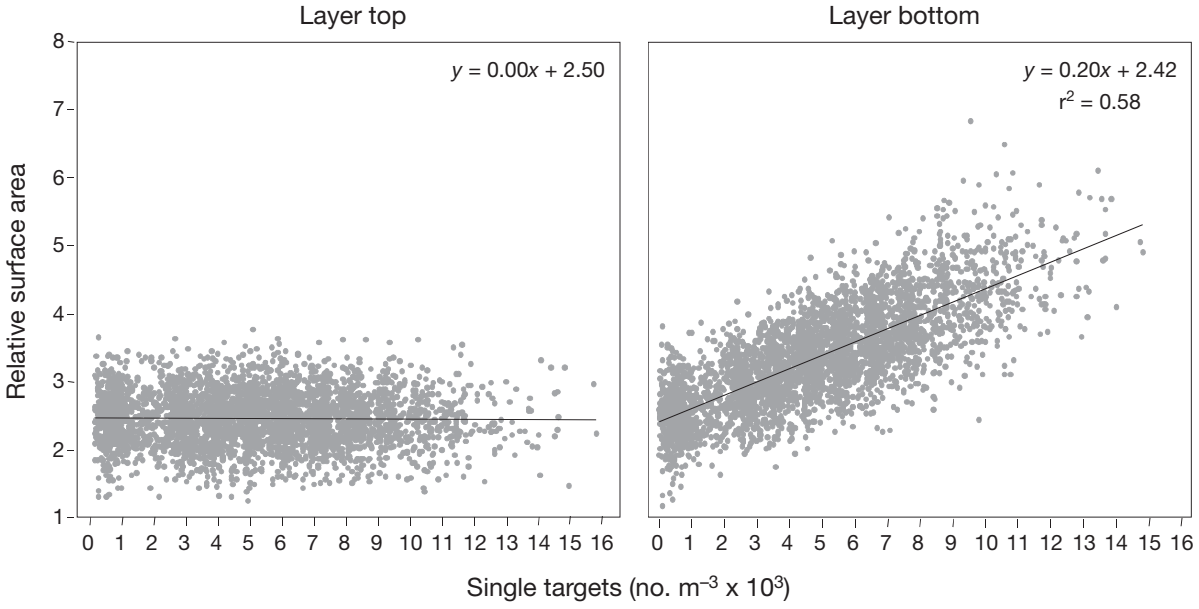

Fig. 6. Relative surface area, a measure of 3-dimensional complexity, of each layer's top edge (left) and bottom edge (right) as a function of fish density. There is no significant relationship between fish density in the 5 m around the layer and the structure of the layer's top edge, but there is a significant, positive, linear relationship between fish density around the layer and the 3-dimensional structure of the bottom edges of layers

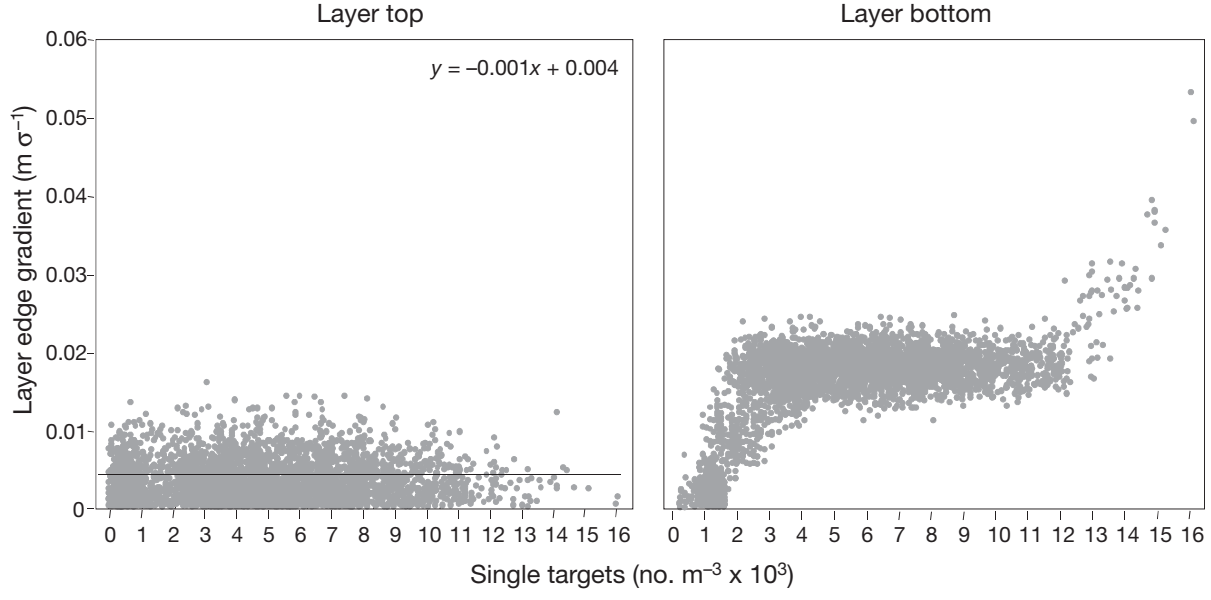

Fig. 7. Steepness of the edge gradients of zooplankton thin layers as a function of the density of fish within 5 m of the layer is shown for each layer's upper (left) and lower (right) edges. Note that the gradient is shown in units of m σ^{-1}, so a value approaching 0 represents a very sharp edge, while a high value represents a diffuse edge gradient. There is no significant relationship between fish density around the layer and the upper edge of layers; however, there is a strong, apparently stepped response in the lower edge gradient with a sharp, linear increase from 0 to 3 fish m^{-3}, a flat but elevated edge gradient value until fish density reached approximately 12 fish m^{-3}, and another sharp, approximately linear increase in edge gradient value as fish density increased further

sent. This response was not linear, however. It appeared to show a threshold response with an increase from 0 to about 3 fish m^{-3}; a flat response between 3 and approximately 12 fish m^{-3}; and then another increase in layer edge gradient when fish density was higher than 12 fish m^{-3}. 1-way ANOVA showed a significant effect of fish density on edge gradient of the layer's bottom edge ($F_{1,2781} = 2.692$; $p < 0.001$).

Discretely bounded decreases in the scattering intensity below the threshold of measurement, holes were observed within identified zooplankton thin layers. There was a significant correlation between the presence of fish and these holes. However, the persistence of these holes after the fish was outside of the layer means that they are not an artifact of the analysis technique or acoustic shadows from the strong targets. Fig. 8 shows the percent of layer area that was hole as a function of the density of single targets within 5 m of the layer and the target strength of those individual targets, an acoustic measurement related to fish size. The percent of layer area that was hole showed a significant increase with increasing target density ($p < 0.001$; $r^2 = 0.77$) and individual target strength ($r^2 = 0.34$; $p < 0.01$). A multiple regression analysis showed that, together, fish density and target strength accounted for more than 91% of the variability in the percent of layer area that was comprised of holes. The mode size of individual holes was 0.5 m^2 and was not significantly affected by the number of single targets ($r^2 = 0.01$; $p > 0.05$) but was affected by the mean individual target strength ($r^2 = 0.57$; $p < 0.01$).

Stationary observations

A total of 1692 acoustic observations of at least 1 min in duration were made when the vessel was keeping station. During these observations, the multibeam echosounder was rotated to achieve 3-dimensional measurements. Layers were present during 52% of these observations. In the August 2006 sampling, the layer detection rate while stationary was 53%, closely matching the rate for underway sampling, likely because the locations for stationary sampling were predetermined. In the July 2006 sampling, the stationary layer detection rate was 50%, much higher than the underway detection rate. This was because the location of stationary sampling sites was not random but rather restricted by other needs of the vessel and guided by data from both the acoustics and optical sampling by other investigators. The depth behavior of single targets that could be tracked for at least 15 s using the split-beam echosounders was analyzed with respect to thin layers. A χ^2 test showed that the depths of single targets consistent with fish were statistically identical to an exponentially decaying distribution tied to the surface ($\chi^2 = 0.37$; n = 1133). When thin layers were present, 2 different distributions were observed. Targets that were first detected above 5 m (n = 268) spent at least 90% of their time within 5 m of the surface. Fish detected below 5 m (n = 951) spent an average of 82% of their time within 2 m of the identified layer. Given the layer thickness and water depth for each observation, if fish were uniformly distributed vertically they would be within 2 m of the layer about 13% of the time. If we assume a random distribution with the midpoint of the water column as the mean, fish would be found within 2 m of the thin layer 7% of

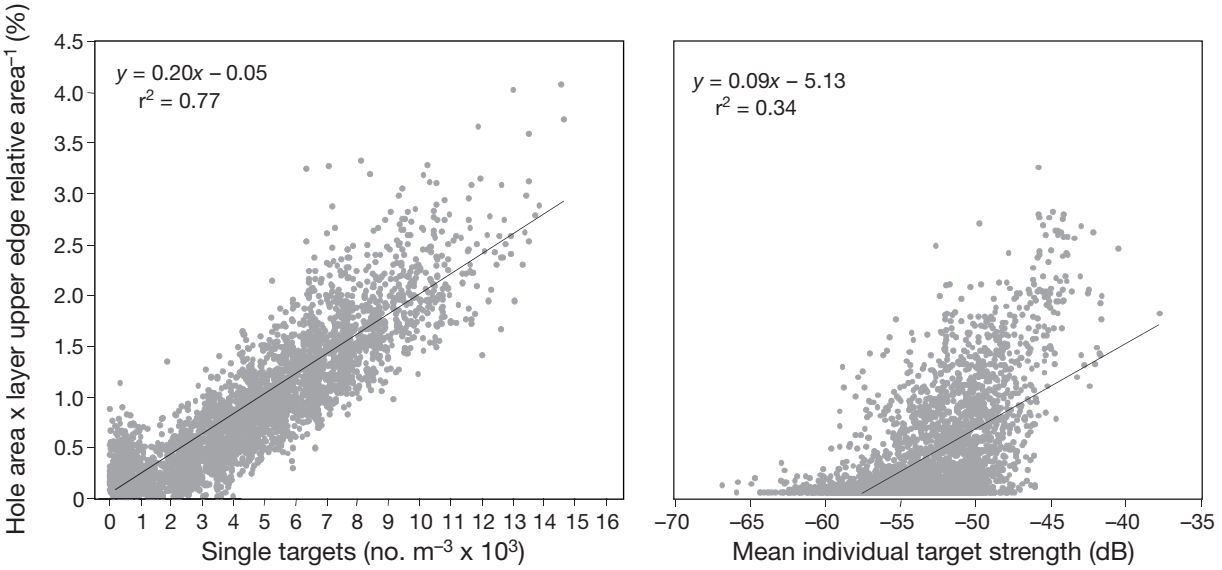

Fig. 8. Percentage of thin zooplankton layer area that is hole as a function of the density of fish in the 5 m around the layer (left) and as a function of the mean target strength of these fish, an acoustic estimate of fish size (right). Each shows a significant, positive relationship despite the fact that the average hole area is not significantly affected by the density of fish, suggesting that more fish lead to more holes in a layer while bigger fish lead to bigger holes in a layer. A multiple regression analysis showed that, together, fish density and target strength accounted for more than 91% of the variability in the % of layer area that was comprised of holes

the time. Finally, if fish were found mostly near the surface with an exponential decay with depth, they would be found within 2 m of the thin layer 15% of the time. Thus fish found below 5 m when thin layers were present spent more time around layers than expected by any model ($\chi^2 < 0.001$, uniform model; $\chi^2 < 0.0005$, random model; $\chi^2 < 0.0001$, exponential decal model). Analyzing only those tracks that were at least 1 min in duration (n = 403) did not change the results, suggesting that the duration of the track did not affect the analysis.

A total of 226 of these stationary observations containing thin layers were at least 20 min in duration. These observations allowed an in-depth analysis of the behavior of fish around layers. Fig. 9 shows a single frame (15 s) from one such observation. See the supplementary data visualization for an observation (approx. 9 min) of a single fish in and around a thin zooplankton layer. This is one example of 136 where the presence of a fish within a thin layer was observed to be associated with the formation of a void or hole in a thin layer. Even from the single frame in Fig. 9, it is easy to detect the obvious hole in the thin layer at the position of the fish. On 53 occasions, the region containing the hole was observed for at least 15 min after the departure of a fish, confirming that these holes are not an artifact of data processing or acoustic shadowing from an intense target. The area of each of these

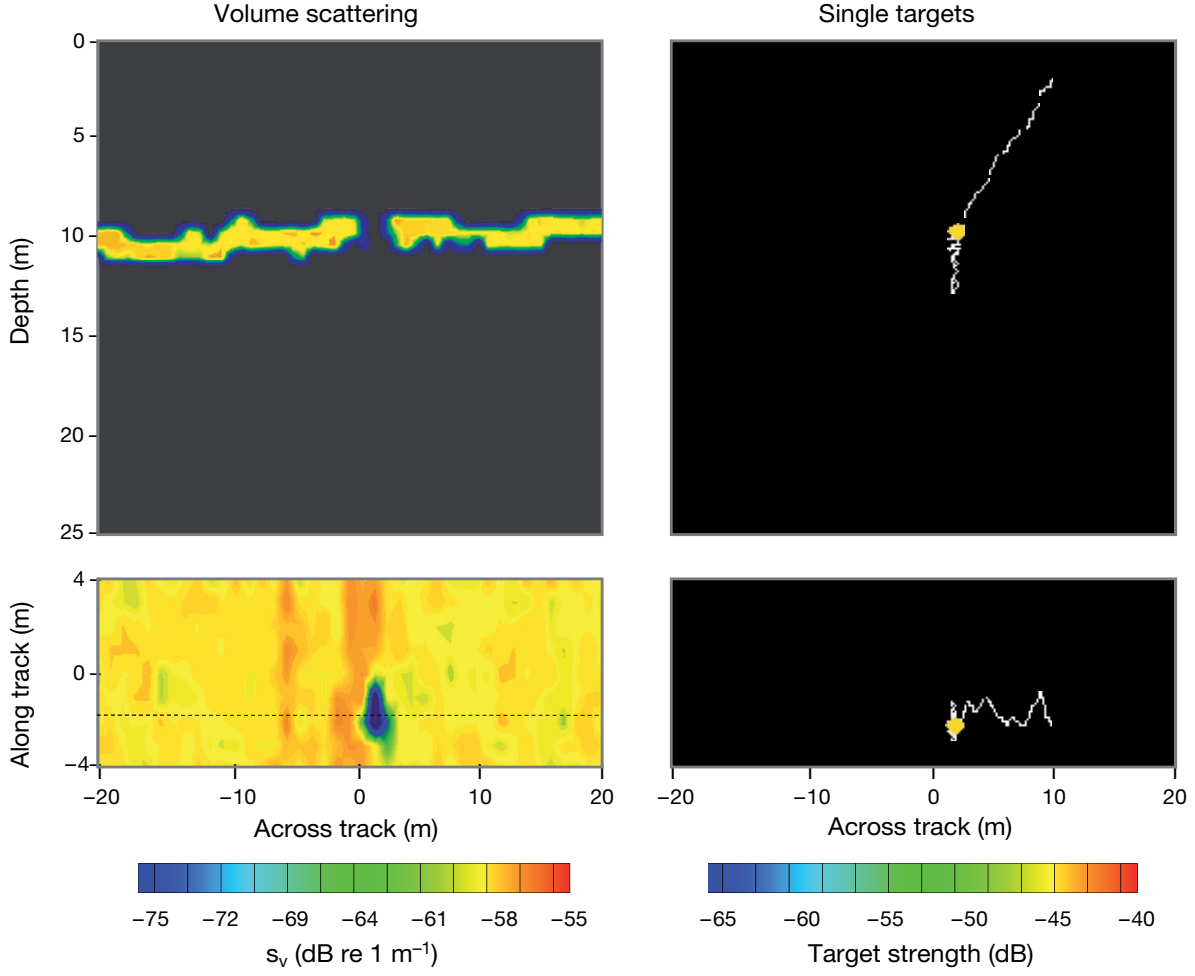

Fig. 9. Data taken at 23:31 h local time of a thin zooplankton layer and an individual fish in Monterey Bay, California. Volume scattering (s_v) from the 200 kHz multibeam echosounder during stationary sampling (left panels), showing the average of 5 echoes covering approximately 1 m along the vessel's path, which were also averaged in 1 m bins across the vessel's path (top left) and a top view of an 8 m swath of these averages integrated over the entire depth of the layer (bottom left). The dotted line at −2 indicates the position of the side-view section shown in the panel above it. The colored dots in the right panels show the position and target strength of an individual target detected with the split-beam echosounder at 38 kHz at the same time as the panels on the left. The white line represents the path of that target from the time it was first detected 3 min earlier than this image. The position of the single target in along-track-depth space (top right) and the position in the across-along-track plane for comparison to the volume scattering data shown on the left (bottom right) are also shown. The entire time sequence of these data can be seen as a data visualization movie in the supplement

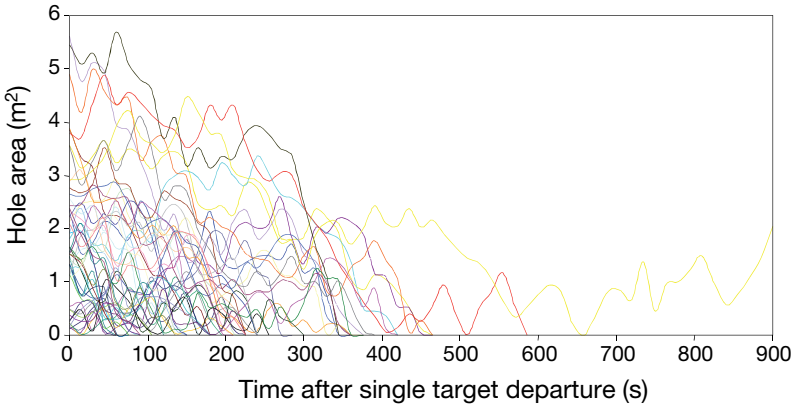

Fig. 10. Area of holes within zooplankton thin layers for 53 regions containing holes that were observed for at least 15 min after the departure of a fish as a function of time after the fish's departure. Each colored line represents the size of an individual hole measured at 15 s intervals. Note that all except one of the holes had closed by the end of the observation period

holes was measured as a function of time and is plotted in Fig. 10. In all but one case, the holes closed within 15 min of the departure of the fish from the layer, with a mean time to closure of just under 4.5 min. In each case, the individual fish approached the layer from underneath, often after diving through it from above, as shown in the observation in the supplementary data visualization.

DISCUSSION

Thin zooplankton layers were relatively common within the study area. Layers were detected more often during the August nighttime sampling than during the July daytime sampling. Because of constraints on the sampling design, the effects of date and time of day cannot be separated. During the July sampling, thin layers of phytoplankton (J. M. Sullivan pers. comm.) and zooplankton (D. V. Holliday pers. comm.) were more common at night than during the day. Optical sampling that covered both the July and August sampling periods showed that thin phytoplankton layers were much more common during the August sampling (M. A. Moline pers. comm.), coincident with a change in the physical regime (M. A. McManus pers. comm.). It is likely that the higher abundance of zooplankton thin layers during the August sampling is thus a combination of both diel and longitudinal changes.

The intensity of volume scattering from thin layers detected acoustically in the present study ranged from –48 to –66 dB at 200 kHz, from –49 to –68 dB at 120 kHz, and from –57 to levels below the –75 dB volume scattering threshold used for analysis at 38 kHz. The volume scattering values at the 2 higher frequencies are quite high for scattering from zooplankton. However, the sharp drop-off in scattering from these layers at 38 kHz and the high abundance of copepods in net tows in areas with these thin layers in comparison to other areas support their classification as zooplankton. The scattering values presented here are comparable to volume scattering measurements at 265 kHz from similar zooplankton scattering layers from Santa Barbara, California, where –50 dB layers were detected (Cheriton et al. 2007) and from Orcas Island, Washington, where –55 dB layers were observed (Holliday et al. 1998). Even more intense scattering has been measured from thin zooplankton layers at higher frequencies (Holliday et al. 2003, McManus et al. 2005, Cheriton et al. 2007). These intense zooplankton scattering layers represent both a significant biomass of animals and a potentially important source of noise for the application of active acoustic systems in habitats containing these thin aggregations of plankton, particularly because their small vertical scales may make their detection difficult with low-resolution sampling techniques.

Layer thickness showed a very strong mode at 2.2 m, with layers consistently thinner than about 3.6 m vertically. This suggests that these intense, vertically compressed features are occurring on a vertical scale distinct from other layered structures commonly seen in acoustic scattering from zooplankton and validating the choice of 5 m to define them operationally. Acoustically identified thin plankton layers were found throughout the water column, which was limited to 20 to 30 m in the study area. Layers detected during underway sampling extended at least 100 m and often were at least 1 km in extent. These extensive layers showed considerable variation in layer depth, thickness, and intensity over their extent.

Data on the 3-dimensional structure of acoustically identified zooplankton thin layers were collected for the first time. These data could be collected very rapidly. For example, during underway sampling a 50 m along-track section of layer at 10 m depth could be assessed in about 20 s with an along-track sampling width of about 40 m. At this depth, the data in raw form have a resolution of about 50 cm along track, 35 cm across track, and 20 cm in depth. During stationary sampling, an 8 m along-track section of a layer at the same depth could be imaged in 15 s before being repeated immediately over the next 15 s. These rapidly repeated stationary observations permitted dynamic analysis of 3-dimensional fish behavior and zooplankton thin layer structure, revealing the behavior of indi-

vidual fish in and around zooplankton thin layers. An example observation can be seen in the supplementary data visualization. Results from this acoustic sampling show that layers have considerable variation in depth, thickness, and intensity across track, even though these data were collected simultaneously at all points along the layer's across-track dimension. Similar variation was observed in layer characteristics in 3-dimensional composite data. This variation in thickness and depth was generally gradual, as would be expected for a coherent feature. These data show that thin layers are not simply flat sheets but at least some of the time can have strong 3-dimensional structure, resulting in layers that look more like mountainous terrain than flat pancakes. This 3-dimensional analysis also revealed that zooplankton thin layers in this habitat were marked by distinctive voids or holes on the scale of 1 m^2. Measurement of these complex, 3-dimensional features and the small holes within them has not been possible with previous approaches for measuring these thin features. This structure has significant implications for understanding the physical and biological processes occurring in and around layers. These results also have implications for interpreting results from instruments that cannot directly assess layer structure in 3 dimensions rapidly.

Acoustic targets consistent with small fish (based on their target strength values and their weak frequency differences) were detected acoustically quite often within the study area. While capture sampling of these fish at appropriately small scales was not possible during acoustic observations, fish were readily observed at the surface and in the mouths of seabirds and sea lions. These sightings indicate that the most common fish within the study area were Pacific sardines, accounting for just over 75% of all visual observations, with the second most abundant fish being northern anchovy, representing about 22% of all visual species identifications. No other species made up more than 1% of all visual sightings. These observations are supported by the catch informally reported by commercial fishermen working in the same area and the commercial landings reported by the California Department of Fish and Game for the greater Monterey Bay area during the study period. Target strength measurements from the literature of Pacific sardines and northern anchovies are limited at 200 kHz. Depending on which data are used, how frequency is corrected for, and what the exact composition of the fish detected was, the estimated lengths of fish detected here would be between 1.1 and 1.8 cm on the small end and between 24.5 and 39.7 cm for fish with the highest target strengths. When only 75% of the values are considered, the length range narrows to between 4.2 and 15.8 cm. This variability in estimated length could be accounted for by the use of only dorsal aspect target strength for the calculation when fish *in situ* are found at a wide range of orientations, introducing substantial variability in target strength-length relationship. Alternatively, the relatively few extreme values may represent scattering from a small number of other, unidentified organisms. The mean length of fish from the acoustics is estimated between 7.8 and 12.5 cm (Love 1971, Barange et al. 1996, Patti et al. 2000, Kinacigil & Sawada 2001), which is consistent with the sizes of fish observed visually and slightly smaller than the sardine and anchovy landings reported by fishermen working the same area.

The depth distribution of fish was strongly affected by the presence of zooplankton thin layers. Fish in the habitat were found mostly near the surface during both daytime and nighttime when there were no zooplankton thin layers. However, when a zooplankton thin layer was present, most fish were found at or very near the depth of the thin layer. This was observed in both the underway and stationary sampling. Two mode depths in the distribution of fish were observed from underway data when thin layers were present: one near the surface and one just slightly deeper than the mode depth for all observed thin layers. Only one mode near the surface was observed when thin layers were absent (Fig. 4). Similarly, depth tracks of individual fish observed in stationary data were tightly coupled to the surface when a thin layer of zooplankton was not observed. This surface-keeping behavior was also observed in about 25% of fish when thin layers were detected. However, the remainder of fish tracks were within 2 m of an identified thin layer an average of 82% of the time, much more than expected by chance given a random, uniform, or surface-coupled depth distribution model. This change in the behavior of fish indicates attraction to thin zooplankton layers in this habitat, suggesting that zooplankton layers are an important resource for fish.

Looking at the depths of individual fish detected during underway sampling relative to the depth of thin layers shows fish behavior in relation to thin layers even more clearly. Fish detected at depths greater than 5 m were nearly all found within 1 m of the bottom edge of a detected layer. This indicates not only that fish were cuing to layers, but also that they were specifically focusing on the bottom edges of layers rather than simply their peaks. This is supported by an examination of the behavior of fish measured using the split-beam echosounders during stationary observations. A total of 287 fish were observed for more than 1 min in and around thin layers. Of these, 285 dove down through a layer, descended 1 to 3 m below it, and then ascended slowly in a spiraling motion through the zooplankton layer (see supplementary data visualization for an example). These fish spent an average 79%

of their time within 1 m of the bottom edge of the thin layer, 54% of their time within 1 m of the peak, and only 19% of their time within 1 m of the upper edge of the layer.

The attraction of fish to zooplankton thin layers leads to the question of how much fish could gain by foraging within thin layers. The density of copepods in layers predicted from zooplankton net tows was about 1000 ind. m^{-3}. This would equate to one copepod every 10 cm on average within a thin layer, while outside of the layers one copepod would be found on average about every 70 cm. The mean layer would have a biomass of copepods of 3 g m^{-3}, while outside of layers copepod biomass would average 0.009 g m^{-3}. This estimate of layer biomass, when converted to biovolume, is similar to that found in Cheriton et al. (2007) for the mean of acoustic layers measured off the Oregon coast but much higher than the layers measured in Monterey Bay during August of 2002. It is important to recognize that we cannot be certain of the composition of the layers identified here since no sampling focused solely on the layers was possible; so these estimates of mean layer numerical density and zooplankton biomass are illustrative only. However, zooplankton thin layers in this study made up 81 to 98% of the total acoustic scattering attributable to zooplankton in the water column, indicating that these zooplankton thin layers would be highly favorable habitat for feeding by zooplanktivorous fish.

From the other perspective, the presence of single targets likely to be fish also had significant effects on zooplankton thin layer structure. An increase in 3-dimensional complexity measured as layer relative surface area was observed on the lower edge of zooplankton thin layers with increasing fish densities (Fig. 6). A decrease in the sharpness of the lower edge gradient of zooplankton was also observed with increasing fish density surrounding the layer, though with a threshold effect rather than a simple linear increase (Fig. 7). While fish appear to be preferentially foraging at the lower edges of layers, the result is opposite to that proposed by Donaghay & Osborn (1997). There were no effects of fish density on the top edges of layers, likely because of the tendency of fish to spend most of their time near the bottom edge of layers rather than the layer's peak or top edge.

Fish were also correlated with the presence of holes in thin zooplankton layers, similar to the correlation of fish with holes in krill layers (Onsrud et al. 2004) and of larger predators with holes in fish aggregations (e.g. Axelsen et al. 2001, Benoit-Bird & Au 2003). Analysis of underway data showed that more fish were correlated with more of the same-sized holes, while bigger fish were correlated with bigger individual holes. All together, these holes accounted for less 5% of layer total area (Fig. 8). Stationary observations support this correlation of fish with holes in the zooplankton thin layers, as holes were repeatedly observed to form in the area surrounding an individual fish swimming up through a zooplankton thin layer. These holes persisted after the departure of the fish, showing that the hole is not simply an acoustical shadow from the strong fish target or an artifact of data analysis. An example of this is shown in Fig. 9. These data cannot be used to examine the direct causes of these holes, but there are several possible alternatives, including grazing losses, mixing caused by fish physically displacing the zooplankton, avoidance behavior by the zooplankton, or a combination of these (e.g. mixing caused by the fish cueing zooplankton avoidance behavior). Observations of the size trajectory of individual holes showed that they typically closed in just under 5 min after the fish associated with the hole left the thin layer. Again, the mechanism of hole closure cannot be examined here. However, the closure of these holes suggests that these zooplankton thin layers are resilient to the level of fish activity observed here.

The resilience of zooplankton layers to fish-created holes indicates that fish are not breaking these zooplankton layers down at large scales. There is also no significant effect of fish density around layers on layer thickness, refuting the initial hypotheses. The data suggest that fish are neither helping to form or maintain layers nor breaking them down with respect to their small vertical scale structure, despite playing a significant role in shaping the bottom edge of thin zooplankton layers and causing holes within the layers. Whether this pattern would hold if fish density were substantially higher remains to be investigated

The present study provides the first measurements of dynamic 3-dimensional characteristics of zooplankton thin layers. The results show that thin zooplankton layers can be quite convoluted at scales of a few meters with small voids or holes on the scale of 1 m^2. The structure of thin zooplankton layers is much more complex than has been revealed by previous approaches for studying these features (see, for example, McManus et al. 2003, Cheriton et al. 2007). This structural complexity has important implications for our understanding of how thin plankton layers are formed and maintained. It also has significant consequences for the interpretation of data collected with instruments that cannot measure this structure at rapid time scales, as there is the potential to alias the data. This is a particular concern if this kind of 3-dimensional structure is also present in the more well-studied thin layers of phytoplankton because of the current absence of optical instruments capable of making measurements of the type made here. It is important to recognize that the potential for the type of 3-dimensional structure within plankton thin layers shown here has not been

missed in previous studies due to errors in sampling strategy, but rather because of the limits of instrumentation. Further exploration of the question of 3-dimensional structure and temporal development at small scales of phytoplankton thin layers will require the development an optical instrument analogous to the multibeam echosounder used here.

Some of the structure observed in zooplankton thin layers was related to the behavior of fish. Fish spent substantially more time within and immediately around thin layers than elsewhere in the water column and modified their typical surface-coupled behavior to spend more time at the depth of thin zooplankton layers when layers were present. This focus by fish of their time and likely their feeding efforts on these features agrees with the results of laboratory studies (Clay et al. 2004) and the conclusion that plankton thin layers can have significant ecological consequences. Holes in layers were strongly associated with the presence of fish, and observations show the appearance of holes in the area immediately surrounding individual small fish, likely sardines and anchovies. Fish spent most of their time near the bottom edges of zooplankton thin layers, typically approaching layers from underneath before spending substantial time within them. The sharpness and 3-dimensional structure of only the lower edges of zooplankton thin layers was significantly affected by the presence of fish. However, fish activity at the densities observed here did not break the layers down at scales larger than about 1 m^2, suggesting resilience of these layers.

In summary, thin zooplankton layers are 3-dimensional features that evolve over time and contain holes within their matrix. This complexity can be partly explained by fish that focused their foraging efforts within these rich resources, indicating significant trophic consequences of these ubiquitous thin layer features. Contrary to the initial hypotheses, however, fish did not either substantially degrade or sharpen thin zooplankton layers. These results have implications for our understanding of the mechanisms that underlie thin layer formation, maintenance, and breakdown, as well as the ecological importance of these features in the coastal ocean.

Acknowledgements. This work was funded by the Office of Naval Research through the Young Investigator Program (N000140510608). James Christmann, the captain of the RV 'Shana Rae' provided exceptional field support. D. Van Holliday, Margaret McManus, and Timothy Cowles began my involvement in the LOCO project and facilitated much of the field-work. James Eckman supported my involvement in the LOCO program to the Office of Naval Research. Percy Donaghay, Mark Moline, and Ian Robbins collaborated on field operations. Ricardo Letelier and the Pacific Islands Fisheries Science Center loaned equipment for the study. Christopher Jones provided the mechanical rotator and wrote code to make it work. Amanda Ashe set up equipment prior to the field effort. Chad Waluk provided technical expertise, assisted with equipment setup and data collection, and participated in preliminary data analysis. Margaret McManus and Amanda Kaltenberg commented on earlier drafts of the manuscript.

LITERATURE CITED

Axelsen BE, Anker NT, Fossum P, Kvamme C, Nøttestad L (2001) Pretty patterns but a simple strategy: predator-prey interactions between juvenile herring and Atlantic puffins observed with multibeam sonar. Can J Zool 79: 1586–1596

Barange M, Hampton I, Soule M (1996) Empirical determination of *in situ* target strengths of three loosely aggregated pelagic fish species. ICES J Mar Sci 53:225–232

Barros NB, Wells RS (1998) Prey and feeding patterns of resident bottlenose dolphins (*Tursiops truncatus*) in Sarasota Bay, Florida. J Mammal 79:1045–1059

Benoit-Bird KJ, Au WWL (2003) Prey dynamics affect foraging by a pelagic predator (*Stenella longirostris*) over a range of spatial and temporal scales. Behav Ecol Sociobiol 53:364–373

Benoit-Bird KJ, Au WWL (2009) Cooperative prey herding by the pelagic dolphin, *Stenella longirostris.* J Acoust Soc Am 125:125–137

Benoit-Bird KJ, Cowles TJ, Wingard CE (2009) Edge gradients provide evidence of ecological interactions in planktonic thin layers. Limnol Oceanogr 54:1382–1392

Beyer JE (1995) Functional heterogeneity: using the interrupted poisson process (IPP) model unit in addressing how food aggregation may affect fish ration. ICES Council Meeting Papers, Copenhagen

Brönmark C, Miner JG (1992) Predator-induced phenotypical change in body morphology in crucian carp. Science 258: 1348–1350

Buckel JA, Fogarty MJ, Conover DO (1999) Foraging habits of bluefish, *Pomatomus saltatrix*, on the U.S. east coast continental shelf. Fish Bull 97:758–775

Burger AE, Wilson RP, Garnier D, Wilson MP (1993) Diving depths, diet, and underwater foraging of rhinoceros auklets in British Columbia. Can J Zool 71:2528–2540

Burkett EE (1995) Marbled murrelet food habits and prey ecology. In: Ralph CJ, Hunt GL Jr., Raphael MG, Piatt JF (eds) General technical reports of the Pacific Southwest Research Station Vol 152, p 223–246

Cairns DK (1987) Diet and foraging ecology of black guillemots in northeastern Hudson Bay. Can J Zool 65: 1257–1263

Cherel Y, Waugh S, Hanchet S (1999) Albatross predation of juvenile southern blue whiting (*Micromesistius australis*) on the Campbell Plateau. N Z J Mar Freshw Res 33: 437–441

Cheriton OM, McManus MM, Holliday DV, Greenlaw CF, Donaghay PL, Cowles TJ (2007) Effects of mesoscale physical processes on thin zooplankton layers at four sites along the west coast of the U.S. Estuaries Coasts 30: 575–590

Clay TW, Bollens SM, Ignoffo TR (2004) The effects of thin layers on the vertical distribution of larval Pacific herring, *Clupea pallasi.* J Exp Mar Biol Ecol 305:171–189

Cooper SD, Walde SJ, Peckarsky BL (1990) Prey exchange rates and the impact of predators on prey populations in streams. Ecology 71:1503–1514

Cowles TJ (2003) Planktonic layers: physical and biological interactions on the small scale. In: Seuront L, Strutton P

(eds) Handbook of scaling methods in aquatic ecology. CRC Press, Boca Raton, p 31–49

De Robertis A, Schell C, Jaffe JS (2003) Acoustic observations of the swimming behavior of the euphasiid *Euphasia pacifica* Hansen. ICES J Mar Sci 60:885–898

Dekshenieks MM, Donaghay PL, Sullivan JM, Rines JEB, Osborn TR, Twardowski MS (2001) Temporal and spatial occurrence of phytoplankton thin layers in relation to physical processes. Mar Ecol Prog Ser 223:61–71

Donaghay PL, Osborn TR (1997) Toward a theory of biological-physical control of harmful algal bloom dynamics and impacts. Limnol Oceanogr 42:1283–1296

Fertl D, Schiro AJ, Peake D (1997) Coordinated feeding by Clymene dolphins (*Stenella clymene*) in the Gulf of Mexico. Aquat Mamm 23:111–112

Fiscus CH, Kajimura H (1981) Food of the Pacific white-sided dolphin, *Lagenorhynchus obliquidens*, Dall's porpoise, *Phocoenoides dalli*, and northern fur seal, *Callorhinus ursinus* off California and Washington. Fish Bull 78: 951–959

Foote KG, Vestnes G, Maclennan DN, Simmonds EJ (1987) Calibration of acoustic instruments for fish density estimation: a practical guide. ICES Coop Res Rep 144

Foote KG, Chu D, Hammar TR, Baldwin KC, Mayer LA, Hufnagle LC Jr, Jech JM (2005) Protocols for calibrating multibeam sonar. J Acoust Soc Am 117:2013–2027

Greene E (1987) Individuals in an osprey colony discriminate between high and low quality information. Nature 329: 239–241

Hildrew AG, Townsend CR (1982) Predators and prey in a patchy environment: a freshwater study. J Anim Ecol 51: 797–815

Holliday DV, Pieper RE, Greenlaw CF, Dawson JK (1998) Acoustical sensing of small scale vertical structures in zooplankton assemblages. Oceanography 11:18–23

Holliday DV, Donaghay PL, Greenlaw CF, McGehee DE, McManus MM, Sullivan JM, Miksis JL (2003) Advances in defining fine- and micro-scale pattern in marine plankton. Aquat Living Resour 16:131–136

Jurvelius J, Knudsen F, Balk H, Marjomaki T and others (2008) Echo-sounding can discriminate between fish and macroinvertebrates in fresh water. Freshw Biol 53: 912–923

Kang M, Furusawa M, Miyashita K (2002) Effective and accurate use of difference in mean volume backscattering strength to identify fish and plankton. ICES J Mar Sci 59: 794–804

Kinacigil HT, Sawada K (2001) Target strength measurements of European anchovy (*Engraulis encrasicolus* L.) by the control method. Acta Adriat 42:103–112

Korneliussen RJ, Ona E (2002) An operational system for processing and visualizing multi-frequency acoustic data. ICES J Mar Sci 59:293–313

Korneliussen RJ, Ona E (2003) Synthetic echograms generated from the relative frequency response. ICES J Mar Sci 60:636–640

Korneliussen RJ, Diner N, Ona E, Fernandes PG (2008) Recommendations for the collection of multi-frequency acoustic data. ICES J Mar Sci 65:982–994

Kratz KW (1996) Effects of stoneflies on local prey populations: mechanisms of impact across prey density. Ecology 77:1573–1585

Krause J, Godin JG (1995) Predator preferences for attacking particular prey group sizes: consequences for predator hunting success and prey predation risk. Anim Behav 50: 465–473

Krebs JR (1978) Optimal foraging: decision rules for predators. In: Krebs JR, Davies NB (eds) Behavioural ecology, an evolutionary approach. Sinauer, Sunderland, p 23–63

Lasker R (1975) Field criteria for the survival of anchovy larvae: the relation between inshore chlorophyll maximum layers and successful first feeding. Fish Bull 73:453–462

Leising AW (2001) Copepod foraging in patchy habitats and thin layers using a 2-D individual-based model. Mar Ecol Prog Ser 216:167–179

Lima SL, Dill LM (1990) Behavioural decisions made under the risk of predation: a review and prospectus. Can J Zool 68:619–640

Love RH (1971) Dorsal-aspect target strength of an individual fish. J Acoust Soc Am 49:816–823

McManus MM, Alldredge AL, Barnard AH, Boss E and others (2003) Characteristics, distribution, and persistence of thin layers over a 48 hour period. Mar Ecol Prog Ser 261:1–19

McManus MM, Cheriton OM, Drake PJ, Holliday DV, Storlazzi CD, Donaghay PL, Greenlaw CF (2005) Effects of physical processes on structure and transport of thin zooplankton layers in the coastal ocean. Mar Ecol Prog Ser 301:199–215

Merrick RL, Chumbley MK, Byrd GV (1997) Diet diversity of Steller sea lions (*Eumetopias jubatus*) and their population decline in Alaska: a potential relationship. Can J Fish Aquat Sci 54:1342–1348

Onsrud M, Kaartvedt S, Rostad A, Klevjer T (2004) Vertical distribution and feeding patterns in fish foraging on the krill *Meganyctiphanes norvegica*. ICES J Mar Sci 61: 1278–1290

Orr MH (1981) Remote acoustic detection of zooplankton response to fluid processes, oceanographic instrumentation, and predators. Can J Fish Aquat Sci 38:1096–1105

Ostrand WD, Coyle KO, Drew GS, Maniscalco JM, Irons DB (1998) Selection of forage-fish schools by murrelets and tufted puffins in Prince William Sound, Alaska. Condor 100:286–297

Patti B, Mazzola S, Calise L, Bonanno A, Buscaino G, Cosimi G (2000) Echo-survey estimates and distribution of small pelagic fish concentrations in the Strait of Sicily during June 1998. GFCM/ SAC Working Group on Small Pelagics, Fuengirola, Spain, 1–3 March 2000

Rines JEB, Donaghay PL, Dekshenieks MM, Sullivan JM, Twardowski MS (2002) Thin layers and camouflage: hidden *Pseudo-nitzschia* populations in a fjord in the San Juan Islands, Washington, USA. Mar Ecol Prog Ser 225: 123–137

Roger C (1994) Relationships among yellowfin and skipjack tuna, their prey-fish and plankton in the tropical western Indian Ocean. Fish Oceanogr 3:133–141

Tamura T, Fujise Y, Shimazake K (1998) Diet of minke whales *Balaenoptera acutorostrata* in the northwestern part of the North Pacific in summer, 1994 and 1995. Fish Sci 64:71–76

Tichy FE, Solli H, Klaveness H (2003) Non-linear effects in a 200-kHz sound beam and the consequences for target-strength measurement. ICES J Mar Sci 60:571–574

Editorial responsibility: Andrew Brierley, St. Andrews, UK

Submitted: December 26, 2008; Accepted: September 10, 2009
Proofs received from author(s): November 17, 2009